

Anomalous Segment Diffusion in Polymer Melts

Matthias Appel, Gerald Fleischer,* and Jörg Kärger

Fakultät für Physik und Geowissenschaften, Universität Leipzig, Linnéstrasse 5, D-04103 Leipzig, Germany

Franz Fujara

Fachbereich Physik, Universität Dortmund, PF 500500, D-44221 Dortmund, Germany

Inyong Chang

Institut für Physikalische Chemie, Universität Mainz, Jakob-Welder-Weg 15, D-55099 Mainz, Germany

Received October 4, 1993; Revised Manuscript Received March 28, 1994*

ABSTRACT: For three high molecular weight samples of poly(dimethylsiloxane), polybutadiene, and polyisoprene the self-diffusion for times smaller than the reptation time T_{rep} was investigated using field gradient NMR in the stray field of a cryomagnet. A time-dependent apparent self-diffusion coefficient D_{app} is observed with time exponents b of the power law $D_{\text{app}} \sim t^b$ between -0.57 and -0.73 . These values are at variance with the strict reptation picture and support more recent theoretical concepts and computer simulations.

Introduction

The tube model of polymer dynamics in the form of the Doi-Edwards theory (DET) is widely accepted for long chains in the melt.¹ A special feature of polymer dynamics is the different time and length scales inherent in the motional process of the chain molecules. In the "classical" picture of the Doi-Edwards theory there are four dynamic regimes which are shown in Figure 1.

There are also deviations of the experimental results from the Doi-Edwards theory;² e.g., the experimentally observed power law exponent of about 3.4 of the dependence of the steady-state viscosity on chain length is not predicted by the DET. Additionally, the interesting crossover from Rouse behavior at short chain lengths to reptation within a temporally stable tube for increasing chain length is not described by the DET. More sophisticated models are needed, and recently different papers on this topic have appeared.³⁻⁶

A sensitive test of theoretical models is the calculation of the time an chain length exponents in the relation between the mean-square displacement of (inner and/or chain end) segments $\langle r^2 \rangle$ and the diffusion time t and chain length N , i.e., the exponents α and β in the relation

$$\langle r \rangle^2 \sim (t/\tau_0)^\alpha N^\beta \quad (1)$$

which are different in different dynamic regimes. τ_0 is a microscopic time constant. In the case of free diffusion the time exponent α is equal to 1. If the diffusion is anomalous or restricted, α becomes smaller than 1, and in the experiment we observe a time-dependent apparent self-diffusion coefficient

$$D_{\text{app}} \equiv \langle r^2 \rangle / 6t \sim t^{\alpha-1} N^\beta \quad (2)$$

The activation energy of D_{app} is reduced to a value of αE_A where E_A denotes the activation energy of the elementary jump process characterized by the time constant τ_0 .

Only a very limited number of experimental methods with appropriate time and space windows are available for investigating the dependence of the segmental mean-

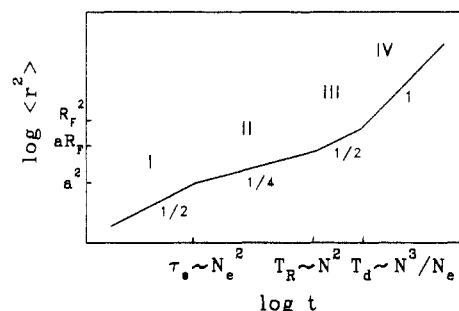


Figure 1. Mean-square displacement $\langle r^2 \rangle$ of polymer segments vs diffusion time t after Doi and Edwards.¹ The different dynamic regimes I-IV and the corresponding crossover times and lengths are indicated. The quantity a denotes the tube diameter.

square displacements $\langle r^2 \rangle$ on time t . One technique is quasielastic neutron scattering (QENS) which has time and space scales in regime I and can reach the crossover to regime II. QENS results have confirmed the lateral constraints of the tube to segmental motions.⁷ A further possibility to monitor the dependence of $\langle r^2 \rangle$ vs t is the measurement of frequency-dependent nuclear magnetic relaxation times,⁸ but the reported results mainly pertain to regimes I and II. Using large field gradients, field gradient NMR allows the observation of the crossover from free diffusion of the coil to restricted diffusion of the segments along or within the tube where the measured self-diffusion coefficient changes from the long-time self-diffusion coefficient D_s of the center of mass of the polymer coil into an apparent self-diffusion coefficient D_{app} . A possibility to increase the field gradient magnitude is the working in the stray field of a cryomagnet as proposed by Kimmich and co-workers,⁹ who very recently reported experimental results on anomalous diffusion in poly(dimethylsiloxane) (PDMS) melts.¹⁰

In this paper we present first results of self-diffusion measurements in polymer melts at the crossover between free diffusion (long-time diffusion) and anomalous diffusion at the space scale $\langle r^2 \rangle^{0.5} < R_F$.

Experimental Method

We use the field gradient NMR in a strong constant magnetic field gradient. The three-pulse stimulated echo (Figure 2) in a magnetic field gradient NMR¹¹⁻¹³ yields the Fourier transform

* Abstract published in *Advance ACS Abstracts*, May 1, 1994.



Figure 2. Pulse sequence $\pi/2 - \tau - \pi/2 - t - \pi/2$ -echo of a stimulated NMR echo experiment. The gradient field is applied permanently.

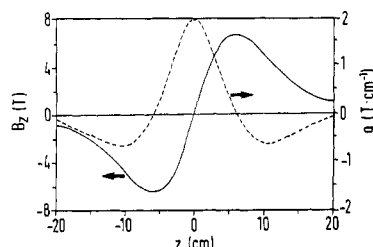


Figure 3. Magnetic field profile (—) and gradient (---) of the Mainz superconducting gradient field. The coordinate represents the location in a vertical room temperature bore of a cryostat relative to the zero field position.

of the self-correlation function of the protons in the system:

$$S = S_0 \exp(-2\tau/T_2) \exp(-t/T_1) \langle e^{-iQr(0)} e^{iQr(t)} \rangle \quad (t \gg \tau) \quad (3)$$

The first two exponentials describe spin-spin and spin-lattice relaxation, whereas the last factor is nothing else than the incoherent intermediate scattering function. Applying a steady field gradient,¹² the generalized "scattering vector" Q is given by

$$Q = \gamma \tau g \quad (4)$$

τ denotes the dephasing time, γ the gyromagnetic ratio, and g the magnetic field gradient. The competing factors of eq 3, the condition $t \gg \tau$, and eq 4 define the working regime of the method. The maximum Q value set in our experiments to be reported in this paper may serve as a numerical example: $Q_{\max} = \gamma \tau g = (2.68 \times 10^8 \text{ T}^{-1} \text{ s}^{-1})(0.002 \text{ s})(95 \text{ T m}^{-1}) = 5 \times 10^7 \text{ m}^{-1}$ such that $1/Q_{\max}$ is of about 20 nm. The dynamic regime extends from a few milliseconds up to a few seconds. Thus field gradient NMR may be considered to be an ideal tool for studying slow polymer dynamics at mesoscopic length scales.

The "key" device for reaching such high magnetic field gradients of sufficient uniformity over the sample volume is a newly installed anti-Helmholtz arrangement of superconducting coils in Mainz (Figure 3). Its design permits a maximum gradient of about 180 T/m at a background field of 2 T or more.¹⁴ The use of such high constant (in time) gradients—as compared to the more conventional pulsed field gradients—implies some new features, advantages (a–c), and potential disadvantages (d–f) which require some comments:

(a) Under favorable circumstances such enormous field gradients allow very high- Q experiments up to more than 0.1 nm⁻¹. Thereby, an overlap with the neutron spin-echo Q regime is established for the first time.

(b) Technically, the common difficulty of equalizing the intensities of the field pulses in the dephasing and rephasing periods does not occur at all.

(c) Further, since no switch on/off delays appear, also small τ values down to a few microseconds can be set. Thus, the method can be applied for studying solid-state diffusion in cases where $T_2 \ll 1 \text{ ms}$.

(d) A disadvantage is due to the gradient strength itself. Because of the limited radio-frequency excitation width, only a thin slice of the sample is at resonance such that the sensitivity of the experiment is significantly reduced. Therefore, it is of utmost importance to use strong and short radio-frequency pulses. Our compromise in the present work consists of 0.4- μs ¹H 90° pulses in a 95 T/m gradient. The polymer melt samples with a high proton density can be measured well by signal accumulation.

(e) Whereas in pulsed field gradient NMR Q is varied by changing the pulse amplitude or its duration, we are bound to change τ which also changes the factor $\exp(-2\tau/T_2)$ (eq 3). This

Table 1. Characteristic Sample Data

	M_w	M_w/M_n	M_e	M_w/M_e	R_F/nm
PDMS ^a	716 000	1.4	12200	58	55
PB ^b	950 000	1.03	2230	426	84
PIP ^b	1 200 000	1.03	5000	120	88

^a From MPI für Polymerforschung Mainz, Germany. ^b From Polymer Laboratories, Ltd., Shropshire, U.K.

potential error source must be carefully considered in the data analysis and/or by reference runs in a $g = 0$ field. In our present work the following procedure has been adopted: The intermediate scattering function is given by $\exp(-Q^2 D_{\text{app}}(t) t)$. Then, for every given t the measured data set $S(Q, t)$ is fitted by $\exp(-2\tau/T_2) \exp(-\tau^2 \gamma^2 g^2 D_{\text{app}}(t) t)$ with two relevant fit parameters, $T_2(t)$ and $D_{\text{app}}(t)$. If the scatter in the T_2 values stays within reasonable limits and T_2 turns out to be t -independent—as it should be of course—a mean value T_2 is extracted. In a second run, the fits are done again keeping T_2 fixed now, thus yielding the final $D_{\text{app}}(t)$ results. Furthermore, all experiments have been limited to $\tau_{\max} < 0.4T_2$; i.e., the transverse magnetization decay is at most 50%. Therefore, we also can disregard the nonexponentiality of the transverse magnetization decay in entangled polymer melts. To verify the fitted T_2 values, we have determined T_2 in separate $g = 0$ experiments, thus obtaining 10 ms at 80 °C for PDMS, 2.8 ms at 72 °C for PB, and 3.5 ms at 92 °C for PI in agreement with the (averaged) fitted values. On the whole we can safely state that within other statistical uncertainties the T_2 decay has been deconvoluted correctly.

(f) A major problem is the extreme sensitivity to building vibrations (<100 Hz) which lead to oscillatory motions of the sample relative to the magnet. Such vibrations produce marked oscillations in $S(Q, t)$ with a Q -dependent amplitude. This artifact sets an upper Q limit: The phase of the NMR signal changes at random if the amplitude of the sample vibrations becomes comparable to Q^{-1} . Quite involving tests led us to now use an appropriate damping setup which ensures the disappearance of any vibration of amplitude of more than about 2 nm, thus leaving the measured curves completely unaffected by this source of error.

To summarize, in spite of the problems which are encountered during the development of this improved technique, we are persuaded that our machine is now able to produce quantitatively correct data of high relevance to be discussed below.

Samples

The recording of segmental diffusion requires polymer samples with a Flory radius $R_F > 1/q_{\max}$, i.e., with R_F on the order of 100 nm and, hence, molecular weights on the order of 10⁶. The reptation time T_{rep} of these samples should be at the long-time edge of the time window of the experiment. Consequently, the use of highly mobile polymers like, e.g., PDMS, polybutadiene (PB), polyisoprene (PI), and polyethylene (PE) or hydrogenated PI (h-PI), is necessary. Since the crossover between the different dynamic regimes is not sharp, it is advantageous to use samples with a small polydispersity. Otherwise, the crossover is additionally broadened by the chain length distribution $w(N)$ of the sample and the experimental $S(Q, t)$ is the sum over the chain length distribution: $S(Q, t) = \int w(N) \exp(-2\tau/T_2(N)) \exp(-Q^2 D_{\text{app}}(t, N) t) dN$, and a simple factorization of eq 3 into a relaxation and diffusion term is no longer possible. The data of our samples are given in Table 1.

Results and Discussion

The results are shown in Figure 4. The experimental time window essentially covers regime III in the DEΓ; cf. Figure 1. The crossover to regime II is expected at $T_R = T_d N_e/N$, and this crossover is at best even reached in our experiments; cf. the data given in Table 1.

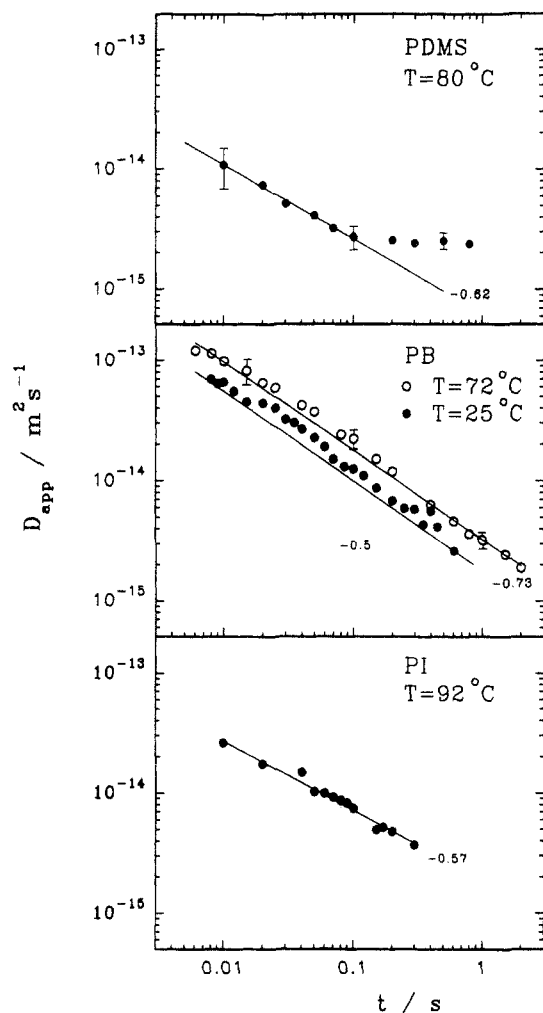


Figure 4. log-log plots of the measured apparent self-diffusion coefficients D_{app} vs the diffusion time t for PDMS, PB, and PI.

For all samples we observe a time-dependent apparent self-diffusion coefficient which obeys a power law $D_{app} \sim t^b$. For the PDMS sample the crossover from anomalous to free long-time self-diffusion is detected. We consider the reptation time T_{rep} a measure of this crossover time. It can be easily estimated from the long-time self-diffusion coefficient D_s and the Flory radius R_F with the relation $T_{rep} = R_F^2/6D_s$. We obtain $T_{rep} \approx 0.2$ s in good agreement with the experiment. Regarding the considerable broad distribution of chain lengths the crossover at T_{rep} is rather sharp. The time exponent b of the relation $D_{app} \sim t^b$ has a value of -0.62 . With this PDMS sample we can demonstrate the relations between T_2 and D_{app} . At short diffusion times the echo attenuation is predominantly determined by the T_2 magnetization decay, and a small uncertainty of T_2 results in a considerable error of D_{app} in the fitting process of the data. As an example, the total echo attenuation of PDMS at $t = 10$ ms and the T_2 decay of the spin echo are shown in Figure 5. One can recognize that very precise T_2 data are necessary to keep the experimental error low at short diffusion times t . For longer t this becomes less important. In our experiments, polymer samples with long T_2 and a high self-diffusion coefficient (e.g., samples at high temperature) should be investigated such that the T_2 magnetization decay becomes small in comparison with the diffusional decay. The typical error bars for PDMS given in Figure 4 lead to the conclusion that PDMS at 80°C is not suited for the aim of the investigation: D_{app} and hence the diffusional decay is too small in comparison with the T_2 decay. Additionally, the chain length distribution is too large and therefore,

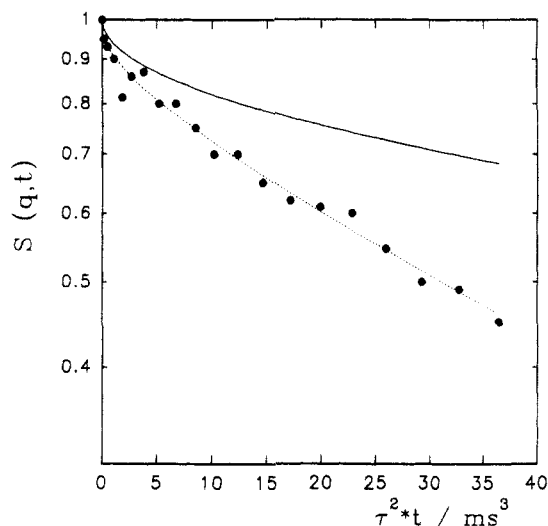


Figure 5. Experimental echo attenuation $S(Q,t)$ for PDMS at $T = 80^\circ\text{C}$ with $t = 10$ ms (\bullet) and the calculated T_2 magnetization decay with $T_2 = 10$ ms as the average value from the fits of all the diffusion times t (—). The dotted line is the fit of the echo attenuation to eq 3 with $T_2 = 10$ ms.

though we detect anomalous diffusion, a tendency toward a deviation from the slope of -0.5 may be stated but cannot be considered to be significant.

The most stable tube exists in the PB sample whose chain length is as long as 426 entanglement chain lengths. D_{app} is almost 1 order of magnitude larger than that for the PDMS sample. Regime III—according to DET—is expected to extend over more than 2 orders of magnitude in time, and this is really observed. At the longest times in the experiment the crossover to long-time diffusion should occur, but this is not precisely to be seen. There exist no reliable long-time self-diffusion data of PB; experiments are in progress in our group. For the PB sample, the time exponent b is found to be -0.73 . Here, the deviation from -0.5 is significant; cf. the error bars in Figure 4.

Due to a shorter T_1 —as compared to PDMS and PB—the PI sample was only measured up to a diffusion time of 0.3 s. Here we obtain for b a value of -0.57 .

From the PB data at 25 and 72°C an apparent activation energy can be calculated. We obtain 9 kJ/mol. According to eq 1, the apparent activation energy of self-diffusion should be the activation energy of free long-time self-diffusion (or, which is the same, of the elementary diffusion step characterized by τ_0) multiplied by the exponent α of eq 1 which is smaller than 1. This decrease of the activation energy is indeed observed. For long-time self-diffusion the activation energy may be assumed to be close to the activation energy of viscosity which is on the order of 30 kJ/mol.¹⁵ With the observed value of $\alpha = 0.28$ this would lead to an apparent $E_A = 8.4$ kJ/mol.

The deviation of the exponent b from the value -0.5 of the DET in the time regime $t < T_{rep}$ is also found in several theoretical concepts. The coupling model of Ngai⁶ assumes that at a distinct time $1/\omega_c$ the relaxation of the chains becomes nonexponential in the form of $Q(t) \sim \exp(-(t/\tau)^{1-n})$ due to the onset of cooperative motions, n being the coupling parameter. More recent results of this model^{16,17} give an exponent α in eq 1 of 0.28 in the limit of a large number of entanglements for the inner monomers of a coil in very good agreement with our experimental results. This is also true for the observed apparent activation energy. The application of the mode-coupling theory to polymer melt dynamics by Schweizer^{3,18} yields the relation $\langle r^2 \rangle \sim t^{3/8} N^{-7/16}$ in the time regime investigated by us, and in a

semiemperical treatment of polymer dynamics in the melt Herman⁵ obtained $\langle r^2 \rangle \sim t^{0.33}$. Both results are in accordance with our experiments within experimental accuracy. Different computer simulations,^{4,19–21} though carried out at an entanglement density of the chains smaller than that of our samples, show also an exponent α smaller than 0.5, and no extended region with $\alpha = 0.5$ is observed when increasing the observation time up to free diffusion.

For each of the three measured samples the exponent b in the power law for D_{app} on t is more negative than the value -0.5 predicted by the DET; i.e., strict reptation within a temporally stable tube in the sense of the Doi–Edwards theory does not seem to take place in our experimental time scale (regime III in DET). The polymer chains seem to have considerable lateral motional freedom. The more recent theories are found to describe the experiments more appropriately. We are convinced that the chains applied in our experiments are long enough to be well entangled. From our first results, a quantitative comparison is scarcely possible. Future experiments are necessary which also have to clarify the dependence on the chain length and, possibly, the influence of the chain length distribution (polydispersity) and temperature.

Acknowledgment. We thank L. Giebel, formerly MPI für Polymerforschung, Mainz, Germany, for the PDMS sample. M.A. thanks for their hospitality the group of Prof. H. Sillescu during a stay in Mainz. F.F. thanks Prof. H. Sillescu, K. Hartmann, G. Diezemann, B. Geil, and G. Hinze for the splendid scientific atmosphere in the Mainz group which has been the most important prerequisite for developing the new gradient NMR spectrometer. Finan-

cial support from the Deutsche Forschungsgemeinschaft (SFB 294) is gratefully acknowledged.

References and Notes

- (1) Doi, M.; Edwards, S. F. *The theory of polymer dynamics*; Clarendon Press: Oxford, U.K., 1986.
- (2) Lodge, T. P.; Rotstein, N. A.; Prager, S. *Adv. Chem. Phys.* **1990**, *LXXII*, 1.
- (3) Schweizer, K. S. *J. Non-Cryst. Solids* **1991**, *191–193*, 643.
- (4) Kremer, K.; Grest, G. S. *J. Chem. Phys.* **1990**, *92*, 5071.
- (5) Herman, M. F. *Macromolecules* **1992**, *25*, 4925.
- (6) Ngai, K. L.; Rendell, R. W.; Rajagopal, A. K.; Teitler, S. *Ann. N.Y. Acad. Sci.* **1985**, *484*, 150.
- (7) Richter, D.; Ewen, B.; Farago, B.; Wagner, T. *Phys. Rev. Lett.* **1989**, *62*, 2140.
- (8) Kimmich, R.; Weber, H. W. *J. Chem. Phys.* **1993**, *98*, 5847.
- (9) Kimmich, R.; Unrath, W.; Schnur, G.; Rommel, E. *J. Magn. Reson.* **1991**, *91*, 136.
- (10) Rommel, R.; Kimmich, R.; Spülbeck, M.; Fatkullin, N. *Progr. Colloid Polym. Sci.* **1993**, *93*, 155.
- (11) Kärger, J.; Pfeifer, H.; Heink, W. *Adv. Magn. Reson.* **1988**, *12*, 1.
- (12) Fleischer, G.; Fajara, F. NMR as a generalized scattering experiment. In *NMR—Basic Principles and Progress*; Kosfeld, R., Blümich, B., Eds.; Springer-Verlag: Berlin, Vol. 30, p 159.
- (13) Fajara, F.; Geil, B.; Sillescu, H.; Fleischer, G. *Z. Phys. B: Condens. Matter* **1992**, *88*, 195.
- (14) Chang, I.; Fajara, F.; Geil, B.; Hinze, G.; Sillescu, H.; Tölle, A. *J. Non-Cryst. Solids*, in press.
- (15) Ferry, J. D. *Viscoelastic properties of polymers*; Wiley: New York, 1970.
- (16) Ngai, K. L.; Skolnik, J. *Macromolecules* **1991**, *24*, 1561.
- (17) Ngai, K. L.; Peng, S. L.; Skolnik, J. *Macromolecules* **1992**, *25*, 2184.
- (18) Schweizer, K. S. *J. Chem. Phys.* **1989**, *91*, 5802, 5822.
- (19) Skolnik, J. *J. Chem. Phys.* **1987**, *86*, 1987.
- (20) Kremer, K.; Grest, G. S. *J. Chem. Phys.* **1990**, *92*, 5071.
- (21) Pakula, T.; Geyler, S. *Macromolecules* **1987**, *20*, 2909.